

# Statistical process control tools for setup reproducibility in quality control practices during nasopharyngeal carcinoma radiotherapy

S. Xu<sup>1,2\*</sup>, Z. Li<sup>1</sup>, J. Hu<sup>1</sup>, J. Zhang<sup>1</sup>

<sup>1</sup>Department of Radiation and Medical Oncology, Hubei Quality Control Center of Radiation Oncology, Zhongnan Hospital of Wuhan University, Wuhan, China

<sup>2</sup>Wuhan University School of Health Sciences, Wuhan, China

## ABSTRACT

### ► Original article

#### \*Corresponding author:

Shifei Xu, MS,

E-mail: xushifei127@163.com

Received: March 2021

Final revised: April 2021

Accepted: May 2021

Int. J. Radiat. Res., April 2022;  
20(2): 299-306

DOI: 10.52547/ijrr.20.2.7

**Keywords:** Statistical process control, QC practice, Setup reproducibility, NPC, Radiotherapy.

**Background:** This study aims to perform quality control (QC) practices for setup reproducibility during radiotherapy for nasopharyngeal carcinoma (NPC) using statistical process control (SPC) tools. **Materials and Methods:** A total of 480 fractional images from 48 NPC patients with the first 10 fractions of the treatment were collected. In QC practices, setup errors were described using the histogram and normal curve, cumulative frequencies of absolute setup errors and 3D Euclidean Distance ( $E_u$ ) were analyzed; the  $\bar{X}$ -S chart and process capability index (Cpk) with the variable  $E_u$  were utilized to identify whether the outlier occurred and to evaluate the QC process. **Results:** The translational setup error distributions were almost normal in Lateral, Longitudinal and Vertical directions and were narrower in Lateral and Vertical directions. Vertical translational errors and  $E_u$  with a larger magnitude sag appeared the most frequently. Between the couch sag and no sag, the  $E_u$  mean of 7 to 7 NPC patients with the same 3 patients was out of control and the standard deviation of  $E_u$  of nil to 2 patients was outlier based on the  $\bar{X}$ -S chart, and the Cpk was 1.05 and 1.36 respectively, when the specification limit of translational errors was  $\pm 3$  mm. **Conclusion:** Daily imaging is necessary to increase setup reproducibility for NPC patients and more measures should be taken to facilitate quality assurance procedures. SPC is better applied to QC practices depending on the reliable data and the acceptable tolerance levels in further studies.

## INTRODUCTION

Despite the radiotherapy complication, patients with nasopharyngeal carcinoma (NPC) have benefited from intensity-modulated radiotherapy (IMRT) technology with good survival outcome over the past decades<sup>(1,2)</sup>. The increasing trueness and precision of the patient setup qualified by setup corrections including translational and rotational errors using daily imaging-guided radiotherapy (IGRT) plays an important role in ensuring that the distribution of the delivered dose conforms to planning target volume (PTV) and clinical target volume (CTV), and the adjacent normal tissue is ultimately spared<sup>(3-5)</sup>. Quality assurance (QA) procedures are critical to accurately deliver radiotherapy. Schubert *et al* stated that the overall procedures governing the use of the image guidance system would affect the setup error measurement<sup>(6)</sup>. Quality control (QC) practices can provide real data to improve QA procedures. Above all, it is essential for us to execute QC practices to increase setup reproducibility during NPC patient radiotherapy.

In radiotherapy, as in other fields<sup>(7-11)</sup>, statistical process control (SPC) and its primal tools provide practitioners with a method of better understanding data. The control chart was initially developed in the late 1920s by Walter Shewhart and eventually disseminated worldwide in 2000s by W. Edwards Deming in industry. To the best of our knowledge, the control chart also called Levey-Jennings chart was first designed in 1950s by Levey and Jennings and applied commonly nowadays in the clinical laboratory<sup>(10,12)</sup>. How do the SPC tools apply for radiation therapy, especially for patient geometric uncertainty? In a literature review, a search of PubMed and Baidu Scholar was done for keywords: statistical process control, control chart, range chart, Levey-Jennings chart and (or) radiotherapy from January 2000 to December 2020. As a result, there were only 10 articles and conference abstracts on setup uncertainty using SPC in radiotherapy, including image registration, anatomical change, setup correction and accuracy, as well as positioning reproducibility. Compared to the number of articles and conference abstracts for radiation therapy using

SPC, the proportion of setup uncertainty in radiation therapy is 14.71% as shown in figure 1. A plethora of papers reports the SPC is applied comprehensively to QC and QA for beam output and symmetry, dose, treatment plan and proton beam range design in radiotherapy, but less for NPC patient setup uncertainty (13-16). This is beyond our expectation, so it necessitates us paying more attention to NPC patient positioning reproducibility using SPC tools. Here, we exclude an article that might be the primary report for radiotherapy planning using SPC by Holli due to earlier publication in 1999 (17).

In QC practices, SPC tools are applicable of detecting errors and making decisions instantly to increase the probability of product quality successfully at lower cost and send ground truth for QA program in industry (7). The same is true of QC practices for setup reproducibility in NPC radiotherapy. Thus, we will initially perform QC practices to maintain and (or) improve setup reproducibility for NPC radiotherapy using SPC tools.

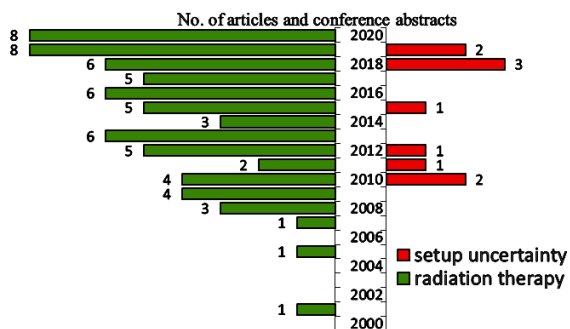


Figure 1. Review and comparison of the number of articles and conference abstracts for setup uncertainty and radiation therapy using SPC.

## MATERIALS AND METHODS

### Patient selection

This retrospective study approved by the medical ethics committee (No. 2017025) enrolled 52 consecutive NPC patients treated with IMRT technology at 6 mega-voltage (MV) energy in our department from October 2019 to November 2020. Helical Direction Tomotherapy (Accuray, Madison, WI, USA) was used to deliver the prescribed dose, which consisted of tomotherapy planning station, the arc-shaped CT detector, the moveable lasers, the couch, and the gantry. Throughout the entire fractionated treatment, 5 patients (2 patients with the weight loss of more than 5%, the bodyweight of one patient less than 30 kg and another patient with the recurrent and metastatic tumor) were excluded when taking into consideration their poor representativeness. Consequently, 48 out of 52 patients were selected in this study: male 32 (66.67%), female 16 (33.33%), age 49.54±12.22 years, body mass index 23.75±3.34 kg/m<sup>2</sup>, Duration

441.03±61.12 s, Couch Travel 21.95 (20.96~23.38) cm, Planed Field Widths 9.75 (9.33~10.30) cm. All patients were diagnosed with non-keratinized squamous cell carcinoma. The prescription dose for each NPC patient treated with concurrent chemotherapy, was 70 Gy in 31 equal fractions. Each patient agreed with the written informed consent.

### CT simulation and planning

At the simulation stage, all patients were immobilized using a head rest, OPTEC™ Fibreplast and Head-Neck thermoplastic masks (Klarity, Guang Zhou, GD, China), with head first and arms placed in pair sides of the body in the prone position. Three-point marks (right and left sides, anterior nasal spine) were placed on the masks as the reference markers for patient setup reproduction. The planning kilo-voltage computed tomography (KVCT) images were carried out by using virtual simulation computed tomography (CT) machine (Sensation Open, SIMENSE, Germany) with the same technical parameters (120 kV, 230 mA, Thickness 3 mm, Pitch 3 mm, Pixel 515×512). The images were transferred to Varian Eclipse Treatment Planning System (Varian Medical Systems, Palo Alto, USA) at 515×512 pixels and were delineated by well-experienced oncologists for gross target volume (GTV), CTV, PTV and organs at risk (OAR) at a base of diagnostic images, such as CT, magnetic resonance imaging (MRI), positron emission tomography (PET) and more. The maximum of the target dose constraints for PTV-GTVp, PTV-CTVp, PTV-CTVn2 were 70 Gy, 60 Gy, 54 Gy, respectively. Regions at risk constraints included brainstem, chiasm, optical nerve, spinal cord, larynx, lens, etc. Data was then transferred to the tomotherapy planning station as per the technical protocol. The default resolution for KVCT image acquisition was 256×256. Finally, a physicist created, calculated and optimized a tomotherapy plan for every patient with the same protocols (fixed plan width 2.512, plan modulated factor 3, pitch 2.087, the margins between PTV and CTV 3~4 mm).

### Image registration

Prior to treatment, all patients were set up by two radiation therapists by aligning the markers on the masks with in-room red moveable lasers. Every patient's daily mega-voltage computed tomography (MVCT) image at 515×512 pixels was acquired to register with the KVCT image by using 3.5 MV photons. The selected slices of MVCT image in the sagittal view determined by oncologists and (or) radiation therapists, included the total target volume. Sometimes parts of it because of the long treatment duration for some patients lack in self-control ability. Anyway, anatomical structures, such as infraorbital rim, nasal septum, clivus, mandibles, cervical vertebra, were selected as the reference point. Acquisition pitch (coarse) and reconstruction interval

(3mm) were chosen for all patients on the scan tab. On the register tab, image alignment between MVCT image and KVCT image was completed by a well-experienced oncologist, a physicist and two radiation therapists using a combination of automatic and manual registration controls. Automatic registration was implemented using the bone technique, super fine resolution, translation only. Manual registration was performed to complement automatic registration based on the image view orientation. After image registration and couch adjustments for translational errors, a scheduled treatment procedure was executed. Please note that rotational errors (Pitch, Roll, Yaw) were not analyzed because of the limited couch shift (18).

**Data collection and analysis**

The data set was obtained from each NPC patient with the first ten fractions (the total of 480 fractional images) by aligning MVCT images with the planning KVCT images. Three-dimensional (3D) coordinate system of positioning corrections defined by the International Electrotechnical Commission (IEC) is depicted in figure 2.

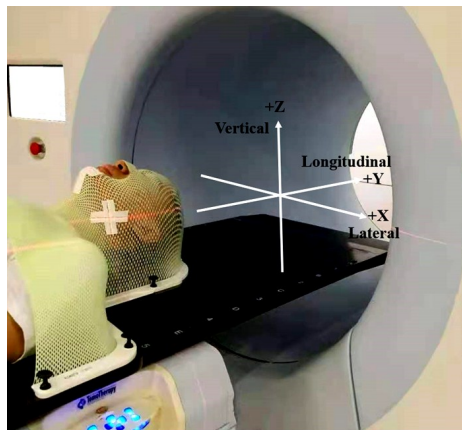


Figure 2. Coordinate system for translation errors.

Data was analyzed using three approaches. Histogram and normal curve were drawn to describe the translational setup error characteristics in Lateral, Longitudinal and Vertical directions. The cumulative frequency of absolute translational errors and 3D Euclidean Metrics (Eu) were calculated to evaluate how often translational errors and Eu occurred with various magnitudes. Eu also called 3D vector lengths represented the total translational variation for every treatment fraction and were calculated using equation 1 as the square root of the quadratic sum of translational shifts in all directions (5,18,19). Setup errors of 5.3 mm were adjusted for the systematic errors caused by the couch sag in Vertical direction. Eu was calculated with and without this adjustment (with the couch sag or not).

$$E_u = \sqrt{T_{Lat}^2 + T_{Lng}^2 + T_{Vrt}^2} \tag{1}$$

Where;  $E_u$ ,  $T_{Lat}$ ,  $T_{Lng}$  and  $T_{Vrt}$ , represented 3D Euclidean Metrics and translational setup errors in Lateral, Longitudinal and Vertical directions.

The  $\bar{X}$ -S chart and process capability index as SPC tools were applied to investigate the NPC patient setup deviation with the variable  $E_u$ . Although numerous control charts were well known and utilized to monitor the process variability (20-25). The  $\bar{X}$ -S chart was applied in this study when considering the large and identical subgroup size  $n=10$  and the fixed sampling interval for each NPC patient (7,9,11,26). The  $\bar{X}$ -S chart could monitor the individual mean  $\bar{X}$  motion and standard deviation (SD) variation and assess whether they were in control or not. The mean and SD represents the central and discrete tendency of data set, respectively (14). In other words, if the mean and SD was out of control limit, the systematic and random errors occurred significantly. Here the  $\bar{X}$ -S chart limits consist of upper control limited (UCL) and central limited (Cl), respectively. Because the less  $E_u$ , the more accurate patient setup. UCL and Cl for the  $\bar{X}$  chart (equations 2 and 3) and the S chart (equations 4 and 5) are expressed as the following formulas (7):

$$UCL_{\bar{x}} = \mu + k \frac{\sigma}{\sqrt{n}} \tag{2}$$

$$CL_{\bar{x}} = \mu \tag{3}$$

$$UCL_s = C_4\sigma + k\sigma\sqrt{1 - C_4^2} \tag{4}$$

$$CL_s = \sigma \tag{5}$$

Where; the  $\mu$  and  $\sigma$  were two parameters of population. A biased constant  $C_4=0.9727$  depending on subgroup size  $n=10$  was the default estimator for the  $\bar{X}$ -S chart, which was tabulated by Montgomery (23,27). The  $\bar{X}$ -S chart had a false-alarm probability of 0.0027 when  $k=3$  and an in-control average run length value of about 370. The  $\mu$  and  $\sigma$  was usually unknown and could be estimated from the  $m$  samples of subgroup size  $n$  as calculated by equations 6 and 7:

$$\mu = \bar{\bar{x}} = \frac{1}{m} \sum_{j=1}^m \bar{x}_j = \frac{1}{mn} \sum_{j=1}^m \sum_{i=1}^n x_i \tag{6}$$

$$\sigma = \frac{\bar{s}}{C_4} = \frac{1}{mC_4} \sum_{j=1}^m s_j \tag{7}$$

Where the  $\bar{X}$  and  $S$  was the estimator of the overall mean and SD of  $E_u$  for all fractions, the  $\bar{x}_j$  and  $s_j$  was the mean and SD of  $E_u$  for the  $j$ -th patient,  $m$  was the number of patients ( $m=48$ ),  $j=1, 2, 3, \dots, m$ .  $n$  was the number of subgroup size for each patient ( $n > 54$ ),  $i=5, 6, 7, \dots, n$ .

The process capability index (Cpk) that

represented the process behavior was utilized to assess the state of QC process. The Cpk demonstrated how data set closed to CL when considering its mean (15,28). If the Cpk was more than 1, the process variation was within the specification limits. If not, more measures should be taken to facilitate the QA procedures and to guarantee the QC process stability. The Cpk was credible when the distribution of the data sets was normal, so the data set was square-root-transformed to mitigate the positive skewness effects on the normality. At present, there was no identical guidance regarding the acceptable tolerance levels among different departments, so three specification limits were exploited based on our clinical practices. The Cpk was calculated using equation 8 to evaluate the QC process stability initially for NPC patient positioning reproducibility.

$$Cpk = \frac{UCL - \mu}{3\sigma} = \frac{C_4(UCL - \bar{X})}{3\bar{S}} \quad (8)$$

Where UCL was the tolerance range upper limit due to the character of  $E_u$ , the  $\bar{X}$  and  $\bar{S}$  was the overall mean and SD for all fractions.

Data is presented in terms of frequency and percentage for categorical variables, the mean±SD for symmetric quantitative variables and the medium (interquartile range, IQR) for skewed ones. The Kolmogorov-Smirnov test was used to test the  $E_u$  normality and translational errors in all directions. Theoretically, translational errors conformed to the standard normal distribution of population N ( $\mu_0=0, \sigma_0^2=1$ ). Compared to the population mean  $\mu_0=0$ , the Student's test was performed to investigate whether the systematic errors appeared in all directions. Because  $E_u$  as an independent variable might be outperformed when translational errors were correlated to each other, the Spearman correlation test was carried out to analyze the correlation of translational errors.

## RESULTS

### Description and analysis of translational setup errors

The characters of translational errors are depicted by histogram and normal curves in figure 3. The mean and SD of translational errors were  $0.15 \pm 1.70$  mm,  $-0.46 \pm 2.44$  mm and  $5.30 \pm 1.77$  mm and the peaks of translational distributions were close to 0 mm, 1 mm, and 5mm in figure 3A, 3B and 3C, respectively. The translational distributions (figure 3A and 3C) were narrower. It is notable that the translational distribution (figure 3C) showed a symmetric offset towards the positive Vertical direction. The normal curves showed the translational symmetrical characteristics at 0 mm (figure 3A, and 3B), 5 mm (figure 3C) and were

narrower (figure 3A and 3C). Generally, the normal curves displayed the normal distribution for translational errors in all directions, although the Kolmogorov-Smirnov test found they were not normally distributed, so was  $E_u$  with sag or no sag. When compared with the population mean  $\mu_0=0$ , there was statistically significant difference in Longitudinal and Vertical directions ( $P < 0.01$ ), but not in Lateral direction ( $P > 0.05$ ). There was a statistical correlation between translational errors in Longitudinal and Vertical directions ( $R^2=0.04, P < 0.01$ ) as shown in figure 4.

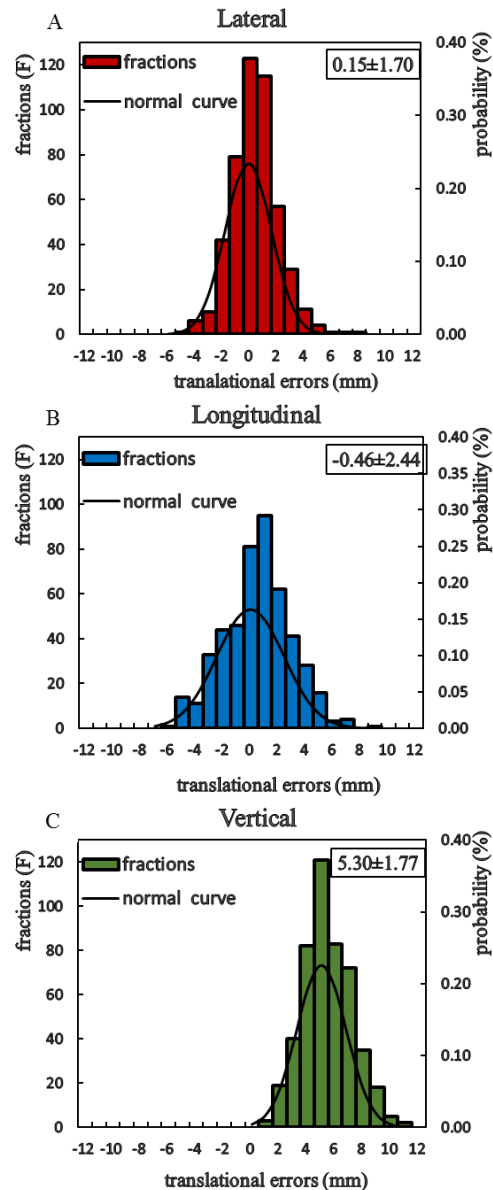
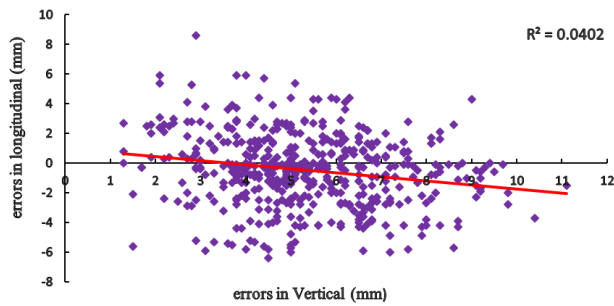


Figure 3. Distributions and normal curves for translational errors (mm) with the mean and truncated at 12 mm.

### Cumulative frequency

Table 1 shows that Vertical translational errors and  $E_u$  with sag of larger magnitude occurred the most frequently, followed by  $E_u$  with no sag, and Lateral and Longitudinal translational errors had the least frequency of appearance. In Lateral and

Longitudinal directions, only 0.42% and 0.42% of treatment fractions were shifted when magnitude was more than 6 mm, whereas this occurred for 33.75%, 49.79% and 5.00% of treatment fractions for Vertical translational shifts and  $E_u$  with sag and no sag, respectively. With magnitudes  $\geq 10$  mm, no treatment fractions were shifted for Lateral and Longitudinal translational shifts and  $E_u$  with no sag but remained for 0.42% and 1.67% of treatment fractions for Vertical translational shifts and  $E_u$  with sag.



**Figure 4.** Spearman correlation analysis between translation errors in Longitudinal and Vertical directions ( $\rho=0.197$ ,  $P<0.001$ ).

**Table 1.** Cumulative frequency (%) of translational errors and  $E_u$  of various magnitudes.

Magnitude (mm)	Translation			$E_u$	
	Lateral	Longitudinal	Vertical	sag	no sag
$\geq 0$	100.00	100.00	100.00	100.00	100.00
$\geq 2$	20.83	41.04	97.71	99.58	73.54
$\geq 4$	2.50	12.71	76.04	90.63	30.63
$\geq 6$	0.42	0.42	33.75	49.79	5.00
$\geq 8$	0.21	0.21	7.71	13.75	0.42
$\geq 10$	0.00	0.00	0.42	1.67	0.00

**The X-S chart**

Figures 5 and 6 demonstrate the mean motion and the SD variation by the X-S chart. UCL and CL for 48 NPC patients with sag and no sag were calculated. When analyzing  $E_u$  with couch sag and no sag for each patient using the X-S chart, we found the  $E_u$  mean of 7 to 7 patients with the same three patients was out of control (figures. 5A and 6A), and the SD of nil to 2 patients was outlier (figures. 5B and 6B), but two outlier points for latter (figure 6B) were very close to UCL. In terms of the outliers, the translational errors for each patient had been shown in table 2. Vertical translation variation for patients with sag was more than that with no sag. After our adjustment, translational errors for four patients (8, 22, 32 45) increased negatively, and translational errors for those patients in Lateral or Longitudinal were larger. This was similar for the same three patients (21 25 30), although they were decreased positively in Vertical direction.

**Process capability index**

Process capability index with and without sag has been displayed in table 3. It was assumed that three specification limits of translational shifts were  $\pm 1, \pm 2,$

$\pm 3$  mm and the range of translational shifts were 0~2, 0~4, 0~6 mm correspondingly in any direction. The Cpk increased with the wider tolerance range of  $E_u$ . The Cpk with sag was less than that with no sag at the same tolerance level. When specification limit was  $\pm 3$  mm and the tolerance range of  $E_u$  was 0~10.39 mm, the Cpk with sag and no sag was 1.05 and 1.36, respectively.

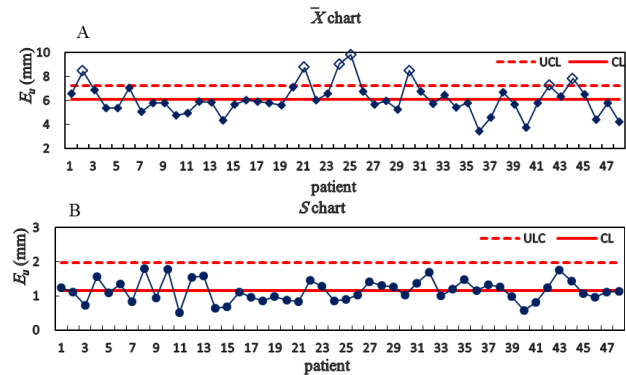


**Figure 5.** Mean motion and the SD variation of  $E_u$  with sag for 48 NPC patients; The open rhombus indicating outlier; UCL: upper control limited; CL: and central limited.

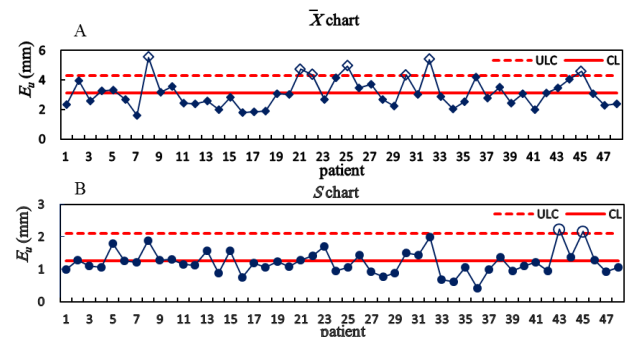


**Figure 6.** Mean motion and the SD variation of  $E_u$  with no sag for 48 NPC patients. The open rhombus and circle indicating outlier, UCL: upper control limited; CL: central limited.

**Table 2.** Translational errors for NPC patient with outlier using two X charts ( $\bar{X} \pm S$ , mm).

patient	Lateral	Longitudinal	Vertical	
			sag	no sag
02 <sup>a</sup>	-1.50±1.97	-0.84±1.93	7.89±0.90	2.59±0.90
08 <sup>b</sup>	-1.22±1.39	4.45±2.28	2.89±0.67	-2.41±0.67
21 <sup>c</sup>	3.21±0.97	-1.32±2.33	7.70±0.75	2.40±0.75
22 <sup>b</sup>	0.68±0.98	-3.84±1.77	4.29±1.06	-1.01±1.06
24 <sup>a</sup>	-0.50±1.32	-0.72±1.93	8.72±0.79	3.42±0.79
25 <sup>c</sup>	0.02±1.78	-2.00±1.21	9.40±0.82	4.10±0.82
30 <sup>c</sup>	1.16±1.95	-1.95±2.71	7.55±0.83	2.25±0.83
32 <sup>b</sup>	2.39±3.87	0.60±2.81	2.92±0.70	-2.83±0.70
42 <sup>a</sup>	-1.02±1.29	-1.61±1.38	6.75±1.39	1.45±1.39
44 <sup>a</sup>	2.04±0.75	-2.73±1.61	6.87±1.28	1.57±1.28
45 <sup>b</sup>	-1.18±1.19	-4.15±2.12	4.35±0.69	-0.95±0.69

Note: a and b represent patients with outlier respectively; c represents the same patient.

**Table 3.** Process capability index with various specification limits.

Specific limit of translation (mm)	Tolerance range of translation (mm)	Tolerance range of $E_u$ (mm)	Cpk	
			sag	no sag
$\pm 1$	0~2	0~3.46	-	0.13
$\pm 2$	0~4	0~6.93	0.25	0.82
$\pm 3$	0~6	0~10.39	1.05	1.36

Note: “-” means null.

## DISCUSSION

The decreasing geometric uncertainty is very critical for accurate radiotherapy. Hence, QC practices must be performed to investigate the patient positional variation. The QC practices introduce an expected object, leading to the need to verify the accuracy of the patient positional reproducibility. SPC and its primal tools have been applied to QC practices and QA procedures in radiotherapy and proved efficiently around 20 years<sup>(17,29)</sup>. However, fewer papers study NPC patient setup reproducibility using  $E_u$ . In this paper, we initially perform QC practices to maintain and (or) improve the NPC patient setup reproducibility using SPC tools.

According to our study, the systematic errors occur in longitudinal direction, and especially in Vertical direction. The reason may be that the top of couch descends towards the positive Vertical and Longitudinal directions when the couch moves from virtual isocenter to the treatment isocenter. A study by Schubert *et al.* suggested that if a pitch offset existed, the restriction would increase the vertical and longitudinal setup correction<sup>(6)</sup>. The correlation between Longitudinal and Vertical translational errors found in our study similarly presents this issue. Meanwhile, the larger random errors appear in the longitudinal direction. The random errors may originate from the head rest because its surface is so curved and smooth that the head and neck shifts more easily in longitudinal direction. The results are in accordance with report delivered by Oh *et al.*<sup>(19)</sup>. At present, daily MVCT is implemented to correct those errors and improve the NPC patient setup reproducibility in our department. In addition, the most frequency of  $E_u$  with sag and Vertical translational errors of the various magnitudes occurred due to the couch sag, and the cumulative frequencies of  $E_u$  with no sag of the same magnitudes decreased sharply. Hou *et al.* reported that the frequency for Vertical translational errors greater than 5 mm was 16.1% for NPC patients; Han *et al.* reported the cumulative frequencies of  $E_u$  and translational corrections with  $\geq 6$  mm to be around 20% and 1.3% for patients with esophageal cancer using the best daily image guidance scenario<sup>(5,30)</sup>. However, in our department, the couch sag range is larger. The excessive extension of the couch may explain this intriguing issue as shown in figure 2. Hence, it is necessary to deal with the couch sag for NPC patient by daily scanning.

The X-S chart intuitively demonstrated the outliers caused by the systematic and random errors. Because of little random variation, we will mainly discuss why the outliers occur by the  $\bar{X}$  chart. The systematic errors caused by the couch sag are attributed to the outliers in Vertical direction. After our adjustment, the outliers occur owing to the systematic errors in Lateral and (or) Longitudinal

direction. Furthermore, Vertical translational errors are adjusted excessively and increase negatively. All the analyses also explain the outliers for the same three patients by the  $\bar{X}$  chart. In addition, our findings suggest that the  $\bar{X}$  chart with sag cannot show the systematic errors well in Lateral and Longitudinal directions, the  $\bar{X}$  chart with no sag bring the expected truth. The results also warn us of the false negative and (or) the false positive positioning errors. However, the  $\bar{X}$  chart helps investigate NPC patient setup deviation. In our literature review, some authors felt that positioning reproducibility, setup correction and anatomical change were studied using the exponentially weighted moving average (EWMA) chart and the cumulative sum (CUSUM) chart because both of them was useful for analyzing data set with the subtle variation<sup>(20-22)</sup>. Others believed that the X chart, the  $\bar{X}$  chart and the X-S chart were utilized to monitor patient setup errors considering the different type of data and the subgroup size<sup>(23-25)</sup>. Moore *et al.* studied the positioning reproducibility for patient with head and neck cancer by the combination of the EWMA and the X charts with variable 3D vector with the advantage of both control charts<sup>(31)</sup>. In this study, our data set that presents a larger variation, especially in Vertical direction, is in accord with the requirement of the X-S chart, similar to the report delivered by Shiraishi *et al.*<sup>(23)</sup>. No matter what control chart is used, we find the remarkable systematic errors and the delicate random errors for individual patient by the X-S chart. Moreover, we initially evaluate the process performance for NPC patient setup reproducibility using the process capability index. The wider the tolerance range of  $E_u$  and translation, the more stable QC process is. However, it only helps recognize the stability of QC process, but does not determine whether the fractionated treatment plan is implemented, because setup errors are corrected by using daily MVCT scanning. Rah *et al.* also reported that the tolerance overdesign tended to suggest the underlying process was overwhelmingly out of tolerance and might not be justified and proposed that it should be redesigned considering the range uncertainties for the proton beam range tolerance<sup>(13)</sup>. Consequently, the QC process stability for NPC patient setup can be judged by using of process capability index.

QC practices are a very important part in radiotherapy because it is useful for detecting errors and giving sufficient evidence for instant remedy<sup>(32)</sup>. In our QC practice, we find the systematic errors for all NPC patients in Longitudinal and Vertical directions and the larger random errors in longitudinal direction, but the errors for individual patient cannot be identified. Fortunately, the X-S chart helps detect the systematic and random deviation for individual patient. QC process is stable with larger specification limit ( $\pm 3$ mm). Based on all these results, daily MVCT imaging is necessary to

improve NPC patient setup reproducibility. Meanwhile, we will take more measures to eliminate the possible sources of setup errors and construct the control chart and calculate the process capability index considering the more reliable data in the future. In doing so, the better SPC tools lead to a more accurate patient positioning reproducibility. This brings great benefits for NPC patients undergoing radiotherapy, for example, reducing the PTV margins, sparing OAR and the adjacent tissues, reducing the concurrent imaging dose with less frequency of IGRT.

In addition, how to design the control chart is always a challenge in all areas (7,14,27). Todd Pawlick *et al.* argued that the limits could be updated when 20–30 subgroups were available (14), but this will increase variability caused by day-to-day factors (the weight loss or gain, tumor deformation and the like). Consequently, the control chart sensibility of is not improved but decreased. More generally, at least 400/ (n–1) samples, where n>1 was the subgroup size, were recommended statistically so that the control chart could perform on average deviation (27). But a prerequisite was that data set was in-control and knowable. We are not aware of the character of the primitive data. Thus, we will study how to create the trustworthy control chart in the further. A limit is that rotational errors are not acquired due to the limited couch shift, a subsequent study aims to perform QC practices with rotation corrections in another medical accelerator using SPC tools.

## CONCLUSIONS

This study demonstrates that SPC and its primary tools can be applied to QC practices for NPC patient positional reproducibility with the couch sag and no sag. Although the random errors vary unremarkably, SPC helps us find the systematic errors in Lateral, Longitudinal and Vertical directions and shows the state of QC process is stable with a specification limit ( $\pm 3\text{mm}$ ). Meanwhile, we must take more measures to improve the QA procedures and increase the setup reproducibility for NPC patients in radiotherapy as soon as possible. We also believe that SPC and its primary tools are better applied to QC practices for NPC patients based on the data set reliability and the acceptable tolerance levels in further studies.

## ACKNOWLEDGMENT

None.

**Conflicts of interest:** Nothing to declare.

**Ethical considerations:** This study was approved by the medical ethics committee of Zhongnan Hospital of Wuhan University, Wuhan, China.

**Author contributions:** (S.X) and (J.Z) made substantial contributions to the study conception and

design, data analysis and interpretation. (J.H) collected the samples. (S.X) and (Z.L) drafted and revised the manuscript. All authors contributed to the work and approved the final manuscript.

**Financial support:** Financial support: This work was supported by Health and Family Planning Commission of Hubei Province of China (WJ2017H0014).

## REFERENCES

- Lam KO, Lee AW, Choi CW, Sze HC, Zietman AL, Hopkins KI, Rosenblatt E (2016) Global Pattern of Nasopharyngeal Cancer: Correlation of Outcome with Access to Radiation Therapy. *Int J Radiat Oncol Biol Phys*, **94**(5): 1106-1112.
- McDowell LJ, Rock K, Xu W, Chan B, Waldron J, Lu L, Ezzat S, Pothier D, Bernstein LJ, So N, Huang SH, Giuliani M, Hope A, O'Sullivan B, Bratman SV, Cho J, Kim J, Jang R, Bayley A, Ringash J (2018) Long-Term Late Toxicity, Quality of Life, and Emotional Distress in Patients with Nasopharyngeal Carcinoma Treated with Intensity Modulated Radiation Therapy. *Int J Radiat Oncol Biol Phys*, **102**(2): 340-352.
- Bell K, Licht N, Rube C, Dzierma Y (2018) Image guidance and positioning accuracy in clinical practice: influence of positioning errors and imaging dose on the real dose distribution for head and neck cancer treatment. *Radiat Oncol*, **13**(1): 190.
- Castelli J, Simon A, Lafond C, Perichon N, Rigaud B, Chajon E, De Bari B, Ozsahin M, Bourhis J, de Crevoisier R (2018) Adaptive radiotherapy for head and neck cancer. *Acta Oncol*, **57**(10): 1284-1292.
- Han C, Schiffner DC, Schultheiss TE, Chen YJ, Liu A, Wong JY (2012) Residual setup errors and dose variations with less-than-daily image guided patient setup in external beam radiotherapy for esophageal cancer. *Radiation Oncol*, **102**(2): 309-314.
- Schubert LK, Westerly DC, Tome WA, Mehta MP, Soisson ET, Mackie TR, Ritter MA, Khuntia D, Harari PM, Paliwal BR (2009) A comprehensive assessment by tumor site of patient setup using daily MVCT imaging from more than 3,800 helical tomotherapy treatments. *Int J Radiat Oncol Biol Phys*, **73**(4):1260-1269.
- Caballero MS (2013) Economic Statistical Design of integrated X-bar-S control chart with Preventive Maintenance and general failure distribution. *Plos One*, **8**(3): e59039.
- Zavridou M, Mastoraki S, Strati A, Tzanikou E, Chimonidou M, Lianidou E (2018) Evaluation of Preanalytical Conditions and Implementation of Quality Control Steps for Reliable Gene Expression and DNA Methylation Analyses in Liquid Biopsies. *Clin Chem*, **64**(10): 1522-1533.
- Vetter TR and Morrice D (2019) Statistical Process Control: No Hits, No Runs, No Errors? *Anesth Analg*, **128**(2): 374-382.
- van den Hoogen LL, Presume J, Romilus I, Mondelus G, Elisme T, Sepulveda N, Stresman G, Druetz T, Ashton RA, Joseph V, Eisele TP, Hamre K, Chang MA, Lemoine JF, Tetteh K, Boncy J, Existe A, Drakeley C, Rogier E (2020) Quality control of multiplex antibody detection in samples from large-scale surveys: the example of malaria in Haiti. *Sci Rep*, **10**(1): 1135.
- Coughlin K, Posencheg M, Orfe L, Zachritz W, Meadow J, Yang K, Christ L (2020) Reducing Variation in the Management of Apnea of Prematurity in the Intensive Care Nursery. *Pediatrics*, **145**(2).
- Levey S and Jennings ER (1950) The use of control charts in the clinical laboratory. *Am J Clin Pathol*, **20**(11):1059-1066.
- Rah JE, Shin D, Manger RP, Kim TH, Oh DH, Kim DY, Kim GY (2018) Tolerance design of patient-specific range QA using the DMAIC framework in proton therapy. *Med Phys*, **45**(2):520-528.
- Pawlicki T, Whitaker M, Boyer AL (2005) Statistical process control for radiotherapy quality assurance. *Med Phys*, **32**(9):2777-2786.
- Chaikh A and Balosso J (2016) Statistical control process to compare and rank treatment plans in radiation oncology: impact of heterogeneity correction on treatment planning in lung cancer. *Transl Lung Cancer Res*, **5**(6):688-694.
- Knutson NC, Samson PP, Hugo GD, Goddu SM, Reynoso FJ, Kavanaugh JA, Mutic S, Moore K, Hilliard J, Cuculich PS, Robinson CG (2019) Radiation Therapy Workflow and Dosimetric Analysis from a Phase 1/2 Trial of Noninvasive Cardiac Radioablation for Ventricular Tachycardia. *Int J Radiat Oncol Biol Phys*, **104**(5): 1114-1123.
- Holli K, Laippala P, Ojala A, Pitkanen M (1999) Quality control in

- health care: an experiment in radiotherapy planning for breast cancer patients after mastectomy. *Int J Radiat Oncol Biol Phys*, **44**(4): 827-833.
18. Contesini M, Guberti M, Sacconi R, Braglia L, Iotti C, Botti A, Abbati E, Lemmi M (2017) Setup errors in patients with head-neck cancer (HNC), treated using the Intensity Modulated Radiation Therapy (IMRT) technique: how it influences the customised immobilisation systems, patient's pain and anxiety. *Radiat Oncol*, **12**(1): 72.
  19. Oh SA, Yea JW, Kang MK, Park JW, Kim SK (2016) Analysis of the Setup Uncertainty and Margin of the Daily ExacTrac 6D Image Guide System for Patients with Brain Tumors. *Plos One*, **11**(3): e151709.
  20. Ung NM and Wee L (2012) Cumulative sum method in nonzero fixed action level setup correction strategy: an application of statistical process control for targeted prostate radiotherapy. *Med Phys*, **39**(5): 2746-2753.
  21. Lowther NJ, Hamilton DA, Kim H, Evans JM, Marsh SH, Louwe RJW (2019) Monitoring anatomical changes of individual patients using statistical process control during head-and-neck radiotherapy. *Physics & Imaging in Radiation Oncology*, **9**: 21-27.
  22. Louwe R and Moore S: OC-0330 (2015) Statistical process control for quality assurance of patient positioning during head-and-neck radiotherapy. *Radiother Oncol*, **115**: S163-S164.
  23. Shiraishi S, Grams MP, Fong DLSL (2018) Image-guided radiotherapy quality control: Statistical process control using image similarity metrics. *Med Phys*, **45**(5):1811-1821.
  24. Govindarajan R, Lluoguera E, Melero A, Molero J, Soler N, Rueda C, Paradinas C (2010) Statistical Process Control (SPC) can help prevent treatment errors without increasing costs in radiotherapy. *Rev Calid Asist*, **25**(5): 281-290.
  25. Xia W and Breen SL (2018) Image registration assessment in radiotherapy image guidance based on control chart monitoring. *J Med Imaging (Bellingham)*, **5**(2): 21221.
  26. Lin YC and Chou CY (2005) On the design of variable sample size and sampling intervals X charts under non-normality. *Int J Prod Econ*.
  27. Saleh NA, Mahmoud MA, Keefe MJ, Woodall WH (2015) The difficulty in designing Shewhart X and X Control charts with estimated parameters. *J Qual Technol*, **47**(2): 127-138.
  28. Mezzenga E, D'Errico V, Sarnelli A, Strigari L, Menghi E, Marcocci F, Bianchini D, Benassi M (2016) Preliminary retrospective analysis of daily tomotherapy output constancy checks using statistical process control. *Plos One*, **11**(2): e147936.
  29. Esposito M, Ghirelli A, Pini S, Alpi P, Barca R, Fondelli S, Grilli LB, Paoletti L, Rossi F, Bastiani P, Russo S (2020) Clinical implementation of 3D in vivo dosimetry for abdominal and pelvic stereotactic treatments. *Radiother Oncol*, **154**: 14-20.
  30. Hou WH, Wang CW, Tsai CL, Hsu FM, Cheng JC (2016) The ratio of weight loss to planning target volume significantly impacts setup errors in nasopharyngeal cancer patients undergoing helical tomotherapy with daily megavoltage computed tomography. *Radiol Oncol*, **50**(4): 427-432.
  31. Moore SJ, Herst PM, Louwe R (2018) Review of the patient positioning reproducibility in head-and-neck radiotherapy using Statistical Process Control. *Radiother Oncol*, **127**(2): 183-189.
  32. Jurković S, Diklić A, Kasabašić M, Radojčić DS, Svabić M, Ivković A, Faj D (2011) Survey of equipment quality control in radiotherapy centres in Croatia: first results. *Arh Hig Rada Toksikol*, **62**(3): 255-260.